

# An experimental investigation of in-plane constraint effect on local fracture resistance of a dissimilar metal welded joint



J. Yang, G.Z. Wang\*, F.Z. Xuan, S.T. Tu, C.J. Liu

Key Laboratory of Pressure Systems and Safety, Ministry of Education, East China University of Science and Technology, Shanghai 200237, China

## ARTICLE INFO

### Article history:

Received 2 May 2013

Accepted 17 July 2013

Available online 26 July 2013

### Keywords:

In-plane constraint

Local fracture resistance

Dissimilar metal welded joint

Fracture mechanism

Safety design

## ABSTRACT

In this paper, an experimental investigation on effect and mechanism of in-plane constraint induced by crack depth on local fracture resistance of two cracks (A508 heat-affected-zone (HAZ) crack and A508/Alloy52M interface crack) located at the weakest region in an Alloy52M dissimilar metal welded joint (DMWJ) between A508 ferritic steel and 316L stainless steel in nuclear power plants has been carried out. The results show that the local fracture resistance of the two cracks is sensitive to in-plane constraint. With increasing in-plane constraint (crack depth  $a/W$ ), the fracture mechanism of the two cracks changes from ductile fracture through mixed ductile and brittle fracture to brittle fracture, and the corresponding crack growth resistance decreases. The crack growth path in the specimens with different in-plane constraints deviates to low-strength material side, and is mainly controlled by local strength mismatch, rather than toughness mismatch. For accurate and reliable safety design and failure assessment of the DMWJ structures, it needs to consider the effects of in-plane constraint on fracture mechanism and local fracture resistance. The new safety design and failure assessment methods incorporating constraint effect need to be developed for the DMWJ structures.

© 2013 Elsevier Ltd. All rights reserved.

## 1. Introduction

Constraint is the resistance of a structure against plastic deformation [1]. According to the crack plane, constraint can be divided into two conditions of in-plane and out-of-plane. The in-plane constraint is directly affected by the specimen dimension in the direction of growing crack, i.e. the length of the un-cracked ligament, whilst the out-of-plane constraint is affected by the specimen dimension parallel to the crack front, i.e. the specimen thickness. As constraint can significantly alter the material's fracture behavior, the effects of in-plane and out-of-plane constraints on local fracture resistance of the homogeneous material have been extensively studied for a long time to increase the accuracy of structural integrity assessment [2–26].

For cracks dominated by linear elastic deformation, the work of Irwin et al. [2] showed that the specimen thickness has considerable effect on the apparent toughness values. The apparent toughness decreases dramatically with thickness until a plateau value of the plane strain fracture toughness is reached. For cracks dominated by plastic deformation, the study of Garwood [3] showed that the experimental  $J$ - $R$  curves obtained from specimens with different geometries and loading modes were different, and the  $J$ -integral resistance curves were considerably affected by constraint. Similar

constraint effects on  $J$ - $R$  curves were observed widely by many other investigators [4–13]. McCabe et al. [4] evaluated the  $J$ - $R$  curve method for fracture toughness characterization using different specimens. Towers et al. [5] investigated the influence of crack depth on fracture toughness. Eisele et al. [6] studied the determination of  $J$ -integral values and crack resistance curves using different methods. Hancock et al. [7] tested a series of cracked specimen configurations to correlate the geometry dependence of crack tip constraint and fracture toughness. Thesis and Bryson [8] studied the influence of crack depth on the fracture toughness of reactor pressure vessel steel. Kirk et al. [9] examined the feasibility of predicting the fracture toughness for structurally relevant situations based on toughness values measured with experimentally convenient specimen geometries. Joyce et al. [10–12] investigated the effect of crack depth and mode of loading on the  $J$ - $R$  curve behavior and fracture toughness of a high-strength steel HY80. Lam et al. [13] used a series of single edge-notched bend (SENB) specimen designs with various levels of crack tip constraint to construct a general expression for a constraint-modified  $J$ - $R$  curve. All experimental results above showed that deeply cracked, bending loaded specimens result in lower  $J$ - $R$  curves, and shallow cracked, predominantly tensile loaded specimens lead to higher  $J$ - $R$  curves. A number of finite-element analyses [14–16] also showed that the crack depth has a significant effect on the stress triaxiality ahead of the crack tip.

Furthermore, different fracture constraint parameters and theories, such as  $K$ - $T$  [17],  $J$ - $Q$  [18,19],  $J$ - $A_2$  [20],  $T_z$  [21–23],  $\phi$  [24,25],

\* Corresponding author. Tel.: +86 021 64252681; fax: +86 021 64253513.

E-mail address: [gzwang@ecust.edu.cn](mailto:gzwang@ecust.edu.cn) (G.Z. Wang).

and  $A_p$  [26], have been developed to characterize and analyze the constraint effect. The  $T$ -stress is an elastic parameter for characterizing crack-tip constraint, and represents the tensile stress acting parallel to the crack plane [17]. The parameter  $Q$  is a constraint parameter quantifying the deviation of opening stress in a non-standard specimen from a standard specimen under elastic–plastic condition, and can effectively describe the constraint effect on the crack-tip field for different geometries under a variety of deformation levels [18,19]. The constraint parameter  $A_2$  is used to relate the first term to the second and third terms of the asymptotic stress distribution in an elastic–plastic cracked body [20]. The  $T_z$  factor introduced by Guo [21–23] is a parameter to characterize the out-of-plane constraint effect accurately. The parameter  $T_z$  can be expressed as follows:

$$T_z = \frac{\sigma_{zz}}{\nu(\sigma_{xx} + \sigma_{yy})} \quad (1)$$

where  $\nu$  is the Poisson's ratio,  $\sigma_{zz}$  the out-of-plane stress,  $\sigma_{xx}$  and  $\sigma_{yy}$  are the in-plane stresses. Variation of this parameter has a marked effect on the size of the plastic region ahead of the crack and on the near tip stress distribution. In order to quantify both the in-plane and out-of-plane constraints, Mostafavi et al. [24,25] defined a new constraint parameter  $\varphi$  which quantified constraint by the areas of the plastic zone at the onset of fracture. Yang et al. [26] defined a parameter  $A_p$  to quantify the constraint by the areas surrounded by the crack-tip equivalent plastic strain ( $\varepsilon_p$ ) isolines for materials with high toughness.

However, the effects of in-plane or out-of-plane constraint on local fracture resistance of highly heterogeneous structures, such as dissimilar metal welded joint (DMWJ), have not been systematically investigated. The DMWJ is indispensable part of structures and has been widely used in primary water systems of pressurized water reactors (PWRs) in nuclear power plants (NPPs). But due to the highly heterogeneous of microstructure, mechanical, thermal and fracture properties and some defects produced during manufacture, the DMWJ is vulnerable component. Different types of defects at different positions within DMWJs have been found in the NPPs of many countries [27,28], and serious leakage events on such DMWJs have also been reported [29,30]. Thus, it is critical and essential to develop an accurate safety design and assessment procedure of structural integrity for the DMWJ's safe service. For doing this, the fracture behaviors of DMWJs under different constraint conditions should be investigated and well-understood.

Wang et al. [31,32] investigated the local  $J$ -resistance curves and fracture mechanism of 13 cracks located at various positions (as shown in Fig. 1) of an Alloy52M DMWJ between A508 ferritic steel and 316L stainless steel (SS). Their results show that the crack 2 at A508 HAZ and the crack 3 at A508/52Mb interface have the lowest  $J$ -resistance curves and are the weakest zones for failure in the DMWJ. In this paper, the two cracks located at the weakest

zones in the Alloy52M DMWJ were selected, and an experimental investigation on the effect and mechanism of in-plane constraint induced by crack depth on local fracture resistance was carried out.

## 2. Experimental procedures

### 2.1. Materials and fabrication of the DMWJ

The Alloy52M DMWJ between A508 ferritic steel and 316L SS in present study is the same as that in the previous studies of authors [31,32], which is used for connecting the safe end to pipe-nozzle of the reactor pressure vessel. The full scale mock up of the DMWJ was detailed in Refs. [31,32], and the four materials composed of the DMWJ joint are shown in Fig. 1. The chemical compositions of the four materials are listed in Table 1 [31,32].

### 2.2. Specimen geometry and crack depth

From the Alloy52M DMWJ of the NPPs, the SENB specimens were machined for measuring the local fracture resistance and observing fracture mechanism. The two weakest positions (the crack 2 and crack 3 in Fig. 1) with the lowest fracture–resistance curves were selected to study the in-plane constraint effect on local fracture resistance. The crack 2 is located in A508 HAZ with a 1.5 mm distance from A508/52Mb interface, and the crack 3 is located in A508/52Mb interface. The specimen thickness  $B$  is 12 mm, the width  $W$  is 14.4 mm ( $W = 1.2B$ ), and the loading span  $S$  is 57.6 mm ( $S = 4W$ ). To investigate the fracture mechanism and fracture resistance under different in-plane constraints, four crack depths denoted as  $a/W = 0.2, 0.3, 0.6$  and  $0.7$  (the SENB specimen with  $a/W = 0.5$  has been studied in the Ref. [32]) were chosen. The loading configuration and geometry of the typical crack 2 specimen ( $W = 14.4$  mm,  $B = 12$  mm, and  $a/W = 0.5$ ) are illustrated in Fig. 2.

The specimens were not side-grooved, an initial notch was prepared by electro-discharge machining, and then a fatigue pre-crack with a length of about 1.5 mm was made in the specimen.

### 2.3. Experiments and observations

The SENB specimens were tested by an Instron screw-driven machine at room temperature. The quasi-static loading was conducted by displacement controlled mode at a cross-head speed of 0.5 mm/min, and the load–load line displacement curves were automatically recorded by a computer aided control system of the testing machine. The single specimen method and the normalization technique conforming the ASTM:E1820 were used to obtain the  $J$ -resistance curve for each specimen, and it has been described in the previous study [32].

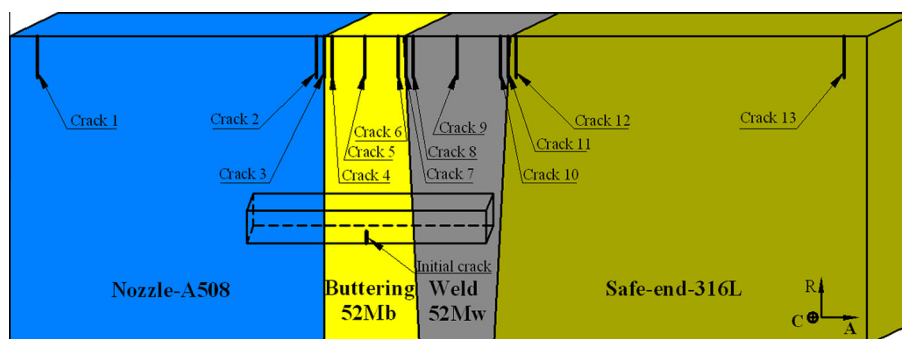


Fig. 1. The four materials composed of the DMWJ and initial crack positions [31,32].

Download English Version:

<https://daneshyari.com/en/article/829781>

Download Persian Version:

<https://daneshyari.com/article/829781>

[Daneshyari.com](https://daneshyari.com)